HITACHI

GE Hitachi Nuclear Energy

Richard E. Kingston
Vice President, ESBWR Licensing

P.O. Box 780
3901 Castle Hayne Road, M/C A-55
Wilmington, NC 28402 USA

T 910.819.6192
F 910.362.6192
rick.kingston@ge.com

Proprietary Notice
This letter forwards proprietary information in accordance with 10CFR2.390. Upon the removal of Enclosure 1, the balance of this letter may be considered non-proprietary.

MFN 08-968

Docket No. 52-010

December 30, 2008

U.S. Nuclear Regulatory Commission
Document Control Desk
Washington, D.C. 20555-0001

Subject: **Response to Portion of NRC RAI Letter No. 185 Related to ESBWR Design Certification Application – DCD Tier 2 Section 3.6 – Protection Against Dynamic Effects Associated With The Postulated Rupture Of Piping; RAI Numbers 3.6-6 S02, 3.6-11 S01, 3.6-12 S01, 3.6-13 S01, 3.6-14 S01, 3.6-15 S01, 3.6-16 S01, 3.6-17 S01**

The purpose of this letter is to submit the GE Hitachi Nuclear Energy (GEH) response to the U.S. Nuclear Regulatory Commission (NRC) Request for Additional Information (RAI) letter number 185 sent by NRC letter dated April 28, 2008 (Reference 1). Previous RAIs and GEH responses are presented in References 2 through 8. RAI Numbers 3.6-6 S02, 3.6-11 S01, 3.6-12 S01,3.6-13 S01, 3.6-14 S01, 3.6-15 S01, 3.6-16 S01, and 3.6-17 S01 are addressed in Enclosure 1.

Enclosure 1 contains GEH proprietary information as defined by 10 CFR 2.390. GEH customarily maintains this information in confidence and withholds it from public disclosure. Enclosure 2 is the non-proprietary version, which does not contain proprietary information and is suitable for public disclosure.

The affidavit contained in Enclosure 3 identifies that the information contained in Enclosure 1 has been handled and classified as proprietary to GEH. GEH hereby requests that the information in Enclosure 1 be withheld from public disclosure in accordance with the provisions of 10 CFR 2.390 and 9.17.

D068
NRO

If you have any questions or require additional information, please contact me.

Sincerely,

Richard E. Kingston

Richard E. Kingston
Vice President, ESBWR Licensing

References:

1. MFN 08-434 from Chandu Patel, Senior Project Manager, ESBWR/ABWR Projects Branch 1, Division of New Reactor Licensing, Office of New Reactors, to Robert E. Brown, *Request for Additional Information Letter No. 185 Related to ESBWR Design Certification Application, 3.6-6 S02, 3.6-11 S01, 3.6-12 S01, 3.6-13 S01, 3.6-14 S01, 3.6-15 S01, 3.6-16 S01, 3.6-17 S01, 3.6-19 S01, 5.4-60 S01, 3.9-19 S04, 3.11-28*, dated April 25, 2008

2. MFN 06-387 from Lawrence Rossbach, Project Manager, ESBWR/ABWR Projects Branch, Division of New Reactor Licensing, Office of Nuclear Reactor Regulation, to David H. Hinds, *Request for Additional Information Letter No. 75 Related to ESBWR Design Certification Application [RAI questions 3.4-1 through 3.4-8, 3.6-20 and 3.6-21, 3.8-108 and 3.8.109, 3.11-1 through 3.11-5, concerning Sections 3.4, 3.6, 3.8 and 3.11 related to the ESBWR Design Control Document, Tier 2, Revision 1, Chapter 3, Structural and Seismic]*, dated October 10, 2006

3. MFN 06-271 from Lawrence Rossbach, Project Manager, ESBWR/ABWR Projects Branch, Division of New Reactor Licensing, Office of Nuclear Reactor Regulation, to David H. Hinds, *Request for Additional Information Letter No. 45 Related to ESBWR Design Certification Application [RAI concerning the evaluation of postulated pipe breaks as described in Section 3.6 of the ESBWR Design Control Document]*, dated August 3, 2006

4. MFN 06-299 from David H. Hinds to the U.S. Nuclear Regulatory Commission, *Response to Portion of NRC Request for Additional Information Letter No. 45 Related to ESBWR Design Certification Application - Protection against Dynamic Effects Associated with the Postulated Rupture of Piping - RAI Numbers 3.6-1 through 3.6-10*, dated August 28, 2006

5. MFN 06-299, Supplement 2 from James C. Kinsey to the U.S. Nuclear Regulatory Commission, *Response to Portion of NRC Request for Additional Information Letter No. 75 Related to ESBWR Design Certification Application - Evaluation of Postulated Pipe Breaks -- RAI 3.6-6 S01*, dated December 14, 2007

6. MFN 06-299, Supplement 3 from James C. Kinsey to the U.S. Nuclear Regulatory Commission, *Response to Portion of NRC Request for Additional Information Letter No. 45 Related to ESBWR Design Certification Application - Line Break Jet Impingement Loads - RAI Numbers 3.6-13 and 3.6-18*, dated February 20, 2008

7. MFN 06-299, Supplement 4 from James C. Kinsey to the U.S. Nuclear Regulatory Commission, *Response to Portion of NRC Request for Additional Information Letter No. 45 Related to ESBWR Design Certification Application - Location of Postulated Pipe Breaks and Postulated Pipe Break Size Dimensions - RAI Numbers 3.6-4 S01 and 3.6-12*, dated February 17, 2008

8. MFN 07-674 from James C. Kinsey to the U.S. Nuclear Regulatory Commission, *Response to Portion of NRC Requests for Additional Information Letter 45 Related to ESBWR Design Certification Application - Evaluation of Postulated Pipe Breaks as described in Section 3.6 of the ESBWR Design Control Document.RAIs 3.6-11, 3.6-14, 3.6-15, 3.6-16, 3.6-17, and 3.6-19*, dated December 14, 2007

Enclosures:

1. Response to Portion of NRC RAI Letter No. 185 Related to ESBWR Design Certification Application – DCD Tier 2 Section 3.6 – Protection Against Dynamic Effects Associated With The Postulated Rupture Of Piping; RAI Numbers 3.6-6 S02, 3.6-11 S01, 3.6-12 S01, 3.6-13 S01, 3.6-14 S01, 3.6-15 S01, 3.6-16 S01, 3.6-17 S01 - Proprietary Version

2. Response to Portion of NRC RAI Letter No. 185 Related to ESBWR Design Certification Application – DCD Tier 2 Section 3.6 – Protection Against Dynamic Effects Associated With The Postulated Rupture Of Piping; RAI Numbers 3.6-6 S02, 3.6-11 S01, 3.6-12 S01, 3.6-13 S01, 3.6-14 S01, 3.6-15 S01, 3.6-16 S01, 3.6-17 S01 – Non-proprietary Version

3. Affidavit

Attachment

1. Yan, Jin, et al, Proceedings of the 16th International Conference on Nuclear Engineering,"Steam Dryer Acoustic Load Predictions in the Main Steam Line Break," ICONE 16-48410

cc:	AE Cubbage	USNRC (with enclosures)
	RE Brown	GEH/Wilmington (with enclosures)
	DH Hinds	GEH/Wilmington (with enclosures)
	eDRF	0000-0093-1135(RAIs 3.6-6 S02, 3.6-11 S01, 3.6-12 S01, 3.6-13 S01, 3.6-14 S01, 3.6-15 S01, 3.6-16 S01, 3.6-17 S01)

Enclosure 2

MFN 08-968

Response to Portion of NRC Request for

Additional Information Letter No. 185

Related to ESBWR Design Certification Application

DCD Tier 2, Section 3.6 - Protection Against Dynamic Effects Associated With The Postulated Rupture Of Piping

RAI Numbers 3.6-6 S02, 3.6-11 S01, 3.6-12 S01, 3.6-13 S01, 3.6-14 S01, 3.6-15 S01, 3.6-16 S01, 3.6-17 S01

Non-Proprietary Version

For historical purposes, the original text of RAI 3.6-6 and previous supplements and the GEH responses are included. The attachments (if any) are not included from the original response to avoid confusion.

NRC RAI 3.6-6

In DCD Tier 2, Rev. 1, Section 3.6.2.2, GE states that blowdown forcing functions are determined by the method specified in Appendix B of ANSI/ANS-58.2. However, GE did not provide any details as to how the blowdown forces are calculated for the ESBWR design, and also did not provide any sample calculation to illustrate the adequacy of any analytical method. Also, there does not appear to be any consideration of how potential feedback between the jet and any nearby reflecting surface(s), which can increase substantially the dynamic jet forces impinging on the nearby target component and the dynamic thrust blowdown forces on the ruptured pipe through resonance, is considered. Provide details (including the methods and computer programs, if any), with examples, for calculating the blowdown forcing functions at break locations that will be used by COL applicant. Also, include a description of how feedback amplification of dynamic blowdown forces will be considered in the calculation.

GE Response

Enclosure 2 provides sample calculations prepared for a typical ABWR Plant for the pipe break forcing functions for main steam pipe break at terminal ends, RPV nozzle and Turbine Stop Valve which is a representative method to be used for ESBWR Plant.

DCD Impact

No DCD change will be made in response to this RAI.

NRC RAI 3.6-6 S01

Part (b) of RAI 3.6-6 was not answered in the GE Response MFN 06-299, dated 8/28/06. Part (b) reads as follows:

(b) Also, include a description of how feedback amplification of dynamic blowdown forces will be considered in the calculation.

This portion dealing with ANS 58.2 issues was deferred pending further discussion. In NRC Letter #75 [MFN 06-387], NRC specified a response date of 11/22/06.

GEH Response

The feedback amplification of dynamic blowdown forces to the broken pipe is calculated by nonlinear time history analysis of the piping system. The calculated time history responses automatically includes the appropriate amplification factors.

The feedback/resonance amplification for jet impingement to the component/structure interacting due to the blowdown loads is accounted for in the analysis by modeling the structure and applying the jet impingement time history load. Also, instead of a dynamic analysis, an equivalent static analysis can be performed with the use of a dynamic load factor as follows:

$F_S = DLF\ (F_{imp\ max})$

Where,

F_S = Equivalent static impingement force

DLF = Dynamic load factor

$F_{imp\ max}$ = Maximum value of the jet impingement force

The impingement force may conservatively be assumed to occur instantaneously and a DLF = 2.0 is used. A separate value for DLF may be analytically established based on DLF = *dynamic deflection/ static deflection* of the object being impinged upon.

DCD Impact

No DCD changes will be made in response to this RAI.

NRC RAI 3.6-6 S02

NRC Summary:

Explain how potential feedback amplification of blowdown force is considered.

NRC Full Text:

GEH provides conflicting answers in its response to RAI 3.6-6 S01, explaining first that feedback amplification of dynamic blowdown forces is calculated using a nonlinear time-history analysis, but then stating that an equivalent static analysis with a dynamic load factor (DLF) may be used instead. GEH uses a DLF of 2. The response is incomplete and unclear. Please explain the following:

(a) Which analysis approach will GEH use, the nonlinear time history or the equivalent static calculations with a dynamic load factor of 2?

(b) If the nonlinear time history analysis will be used, what tools are employed? How have they been validated and certified? What are the bias errors and uncertainties associated with the tools? Also, how is the time-varying jet impingement loads simulated?

(c) If the static analysis approach is used, GEH is requested to respond to the follow-up RAI 3.6-14 S01, which addresses similar concerns the staff has with the response to this RAI concerning the use of DLF of 2.

GEH Response

(a) The analysis approach that will be used is described below. Tables 1 and 2 provide terminal end break locations for inside and outside the containment respectively. Figures 1, 2 and 3 provide information as to the location of reactor pressure vessel nozzles and required pipe break locations.

Pipe Breaks inside Containment (See Table 1 for the list of terminal end breaks)

Terminal end break locations:

- The main steam (MS) pipe nozzle at the reactor pressure vessel (RPV) penetrates the reactor shield wall (RSW) penetration. The break is located outside the RSW where nozzle is welded to the 30" diameter pipe. The MS line terminal end break locations are shown in Figure 5 and the potential jet interaction to the gravity driven cooling system (GDCS) pool wall from the MS nozzle break is shown in Figure 4.

- 2" diameter reactor water clean-up nozzle (RWCU) and 1-1/4" diameter control rod drive (CRD) pipe terminal end breaks are located at the RPV bottom.
- All other terminal end breaks at the RPV nozzles (see Table 1) are confined in the annulus region that is between the RPV and RSW.

The radial distance between the RPV outer surface and the inner surface of RSW is 908 mm (approximately 3 ft.). The RSW is a 160 mm (6.3") thick cylindrical steel structure having penetrations through which piping systems connect to the RPV nozzles.

Analysis Approach:

- Main steam line terminal end breaks (RPV nozzle, 30" dia.) jet blowdown force calculation for the inside containment will be analyzed using CFX (a CFD software package). The CFD transient nonlinear analysis will determine jet pressure on targets and the total jet force can be evaluated. The program will capture reflective shock wave and feedback amplifications of jet blowdown on a target.

The following analytical steps are involved:

1. RELAP 5 program will be used to determine the "thrust force" and jet flow time history.
2. The ruptured piping will be modeled in ANSYS and based on the "thrust force" simulation for the ruptured pipe condition in the ANSYS analysis, the deflections of the broken pipe end and the load reaction at the pipe rupture support are determined.
3. Computational Fluid Dynamic (CFD- ANSYS CFX 10.0) program will be used to model the jet flow time-history and the deflected pipe of the broken pipe to assess the pressure time history (also, force time history) of the jet and the maximum force on a target. This analysis will capture the feedback amplification, the jet unsteadiness, jet reflection, turbulence, and compressibility characteristics of the jet.
4. The interacting structure is then modeled with the appropriate boundary conditions and applying the force time history as the input forcing function (obtained from CFD analysis), a dynamic analysis is performed. The structural responses are evaluated in accordance with the design requirements. The dynamic analysis is performed by ANSYS or other GEH approved structural analysis program.
5. Rupture supports will be used for the MS lines. The pipe rupture reaction at the support will be obtained from the ANSYS analysis.

All other terminal end breaks inside containment are located at the RPV nozzles that are confined between the RPV and RSW (see Table 1) except the 2" diameter reactor water clean-up (RWCU) and 1-1/4" diameter control rod drive (CRD) piping. These terminal end breaks are described below:

- For 12" diameter feedwater (FW) piping terminal end breaks (see Figure 6), the evaluation will be performed similar to the main steam analysis method. Jet impingement effects onto the RSW and RPV supports will be evaluated and the piping will be supported by rupture restraints.

- For 12" diameter reactor water clean-up (RWCU) piping terminal end breaks (see Figure 7), the evaluation will be performed similar to the main steam analysis method. Jet impingement effects onto the RSW and RPV supports will be evaluated and the piping will be supported by rupture restraints.
- The 18" diameter isolation condenser (IC) piping nozzle at the RPV is connected with a small pipe spool that is attached to two depressurization valves (DPVs). The terminal end break at the 18" nozzle is contained in the annulus region, and the piping will be supported by rupture restraints. The blowdown reaction load to the RPV of the 18" IC nozzle terminal end break (see Figure 8) is enveloped by the MS nozzle break evaluation results as the MS line break contributes the largest reaction load on the RPV and RSW structure.
- The piping associated with the 8" diameter IC return nozzles (total 4 nozzles), the lines are connected to the IC condensers. During normal plant operation, these lines are closed and contain water in the lines. Also, due to the in-line valve being normally closed, the piping between the nozzle and the valve (10 ft. approx) will contain limited water inventory; and hence, the small volume will rapidly release the pressure and energy contained in the pipe side of the rupture. For break at the RPV nozzles (see Figure 8) and at the pipe end, an equivalent static analysis method will be used for the thrust force calculation (see formula in response to item C). The standard pipe support structures will adequately resist the pipe break thrust force.
- There are eight (8), 6" diameter gravity driven cooling system (GDCS) nozzles and there are (4), 6" diameter equalizing GDCS nozzles connect to the RPV. The piping is routed from the RPV to squib valves that are normally closed and there is no flow in these lines. The piping with static head pressure of pool water (temperature, 122 F) will remain in the sub-cooled state. Additionally, because of the inline squib valve (normally closed), the piping between the nozzle and the squib valve (20 to 30 feet approx) will contain limited water inventory; and hence, the small volume will rapidly release the pressure and energy contained in the pipe side of the rupture. For a break at the RPV nozzle (see Figure 9) and at the pipe end, an equivalent static analysis method will be used for the thrust force calculation (see formula in response to item C). The standard pipe support structures will adequately resist the pipe break thrust force.
- The terminal end breaks (see Figure 10) at the 2" diameter stand-by liquid control (SLC) and 2" diameter head vent pipe break (see Figure 11) inside the annular space between the RPV and RSW, the pipe rupture evaluation will be performed by static analysis method since the mass/energy release is considerably less than other large RPV nozzle breaks. The effects from the rupture of these nozzles are insignificant. This piping does not function during normal operation and is isolated from the RPV by a normally closed valve. An equivalent static analysis method for thrust force calculation will be performed (see response to item C). The standard pipe support structures will adequately resist the pipe break thrust force.

  The 2" diameter head vent line from the RPV splits into two segments via a TEE connection. The piping from one end of this TEE connects to the main steam line A. The piping will be rigidly supported such that pipe deflection remains minimal. In the

event this piping is decoupled from the large bore analysis and a terminal end break is postulated at the 2" to 30" connection, the jet impingement effects will be insignificant as the piping will be adequately restrained. If the piping is modeled with the main steam line system, a break is not postulated.

An equivalent static analysis method for thrust force calculation will be performed (see response to item C) and the standard pipe support structures will adequately resists the pipe break thrust force.

The piping from other end of the TEE having two inline normally closed valves ends at the drywell sump. This line is only used for the reactor hydro testing purposes and the system is functional less than 1% of the life of the plant; and therefore, a rupture evaluation is not required.

- There are four (4) 2" diameters RWCU drain piping nozzles attached to the bottom shell of the RPV (see Figure. 7). The nozzles are installed in an angle pointing outward from the surface of the RPV bottom spherical shell. For terminal end break at the nozzles, the jet impinges to the RPV pedestal structure and on the basemat and these interactions from small pipe break jet force are acceptable. The pipe whip or jet interaction from the 2" diameter connecting pipe, these interactions with the surrounding CRD housings are acceptable since these housings are larger in size (6" diameter) and have a substantially thicker wall.

  An equivalent static analysis method for thrust force calculation will be performed (see response to item C) and the standard pipe support structures will adequately resists the pipe break thrust force.

- There are four (4) 2" diameter nozzles at the RPV of the Reactor Vessel Level Instrument System (RVLIS) piping system where terminal end breaks are postulated (see Figure 11). The RVLIS piping system measure the water level of the RPV. These 2" diameter nozzles are located in the annulus. The piping connected to these nozzles is of 1" diameter pipe. The effects from the rupture of these nozzles are insignificant.

  An equivalent static analysis method for thrust force calculation will be performed (see response to item C) and the standard pipe support structures will adequately resists the pipe break thrust force.

- The evaluation for the CRD piping (1-1/4" diameter) is provided in the DCD Tier 2 subsection 3.6.2.1.3. The break location are shown in Figure 12.

Pipe Breaks Outside Containment (See Table 2 for the list of terminal end breaks)

For terminal end breaks in piping outside the containment, the postulation will be as follows:

- 30" diameter MS line breaks (see Figure 5) at the header near Turbine Stop Valve (TSV) located in Turbine Building will be computer analyzed and piping will be restrained. This break will be analyzed using the CFD program that will include the force time history.
- 24" diameter FW line breaks at FW heaters (see Figure 6) are located in Turbine building. FW heaters are located in concrete enclosures. Pipe rupture restraints may be required for FW line terminal end breaks in turbine building. There are no safety related targets in the enclosure. MS piping analysis results may envelop the pipe rupture reaction load for these breaks. If a similarity in the piping geometry between the MS and FW line breaks are not established, a CFD analysis approach as discussed earlier for the MS breaks will be performed for the FW line breaks.
- The 6" and 8" diameter RWCU line break at the Regenerative HX and 12" diameter RWCU line break at the non-regenerative HX are located in the Reactor building (see Figure 7). Terminal end breaks at the non-regenerative Heat Exchanger (nozzles) located in a separate room that will not require a non-linear time history analysis for jet impingement evaluation. Safety related targets are not located in the rooms. Similarly, terminal end breaks at 8" and 12" nozzles (see Figure 7) at the RWCU pumps (Inlet and outlet) are located in a separate room. There are no safety related targets identified in the pump room.

  Note that the 12" RWCU piping will be analyzed using computer codes - RELAP, ANSYS, and CFD programs. The piping will be modeled from RPV nozzle up to regenerative HX nozzle. As stated above, the other RWCU breaks are located in separate rooms where there are no SSCs.

  The thrust force loads resulting from other RWCU breaks (see Figure 7) can be determined by an equivalent static analysis method. The standard pipe support structures will adequately resists the pipe break thrust force.
- The piping associated with the terminal end breaks at the 8" and12" diameter RWCU pump outlet nozzles and 6" diameter demineralizer tank inlet and outlet nozzles (see Figure 7) contain highly radiated low temperature (120 °F) water. Due to the high radiation, these components (Hx, pumps, demineralizer tank) are placed in separate rooms/cubicles where no other SSCs are located. Therefore, there is no concern for the pipe whip or jet impingement interaction to any SSCs from these terminal end breaks. The thrust force for these breaks can be determined using the equivalent static analysis method.
- The Standby Liquid Control accumulators are located in a separate room in the reactor building. The segment of piping between the accumulator vessel and the

Squib valves, which remains normally closed, is a cold (80 °F) piping. Therefore, the piping system doesn't have internal thermal energy. The piping length between the nozzle and the in-line squib valve is approximately 20 ft. The nozzle is located at the bottom of the tank. The break at the nozzle (see Figure 10) will result in draining the high-pressure borated water onto the floor. There are no safety related components located in the room. The thrust force for these breaks can be determined using the equivalent static analysis method.

- The 6" and 4" terminal end breaks (see Figure 8) at the Isolation Condenser HX nozzles are located inside the IC/PCCS pool and are submerged. Each IC HX is in a separate pool that does not have any other equipment inside the pool. The steam flow from this break rapidly condenses in the surrounding water and remains in the pool. These breaks do not result in a direct jet impingement on any safety related target.
- The evaluation for the CRD piping (1-1/4" diameter) is provided in the DCD Tier 2 subsection 3.6.2.1.3. Refer to Figure 12 for break location at the hydraulic control unit (HCU) nozzles.

[[

]]

Note: See the attached technical proceeding (ICONE 16-48410), Titled: "Steam Dryer Acoustic Load Predictions in the Main Steam Line Break Event" by Jin Yan et. el. of GEH (Attachment 1). [[

]]

(c) The equivalent static analysis method will be used to determine jet force for the following break locations:

Inside Containment

- All 2" diameter piping at the RPV nozzles between the RPV and RSW

Justification: An equivalent simple static method for the jet load calculation is acceptable (see thrust force calculation formula as shown below). The thrust force reaction to RPV and RSW are enveloped by the large break results from 30" MS and/or 12" FW breaks. Standard pipe supports will adequately restrain the pipe rupture thrust load.

- 6" GDCS nozzles and 8" IC return line:

Justification: A simple equivalent static method for the jet load calculation is acceptable (see thrust force calculation formula and the ANS 58.2 guidance as shown below). The thrust force reaction to RPV and RSW are enveloped by the large break results from 30" MS and/or 12" FW breaks.

- 2" RWCU Drain line at the RPV bottom:

Justification: The blowdown force will be calculated by equivalent static method (see below) as the break size can be categorized as a small break. Jet impingement interaction to RPV pedestal and concrete basemat below the RPV is acceptable.

Outside Containment:

- The jet blowdown force (thrust force) for all breaks except for the MS, FW, and RWCU piping will be analyzed using an equivalent static analysis method (see thrust force calculation method below).

  Justification:
  For RWCU pump and demineralizer tank nozzle breaks the thermal energy associated with these lines are insignificant (line temp. = 120 °F). A DLF =2.0 may be used to determine a conservative thrust force. The RWCU pump and demineralizer tank are located in a separate room and no other safety-related component, which are required for safe shutdown of the reactor, will be located in these rooms.

  For 3" diameter SLC line and 6" & 4" IC/PCCS piping– see outside containment pipe break evaluations. There are no other safety-related components, which are required for safe shutdown of the reactor will be located in the SLC tank rooms or in IC/PCCS pool.

Thrust force is determined as follows:

$F_S = DLF^* (F_{imp\ max})$

Where,

F_S = Equivalent static impingement force

DLF = Dynamic load factor

$F_{imp\ max}$ = Maximum value of the jet impingement force

DLF = 2.0 is conservative unless a lower value is analytically justified (see Attachment 2).

[For an equivalent static analysis of the target structure, the jet impingement force is multiplied by a dynamic load factor of 1.2 to 2.0, depending upon the time variance of the jet load and the elastic/plastic behavior of the target. This factor assumes that the target can be represented as essentially a one-degree-of-freedom system.]

The guidance provided by ANS 58.2 Section 6.2.4 is as follows:

"For closed-ended piping runs, depending upon the proximity of the closed ended (dead end or normally closed valves) to the postulated break, if it can be shown that the stored energy is insufficient to cause pipe whip, further pipe whip evaluation need not be considered".

TABLE 1

[[

]]

[[

]]

TABLE 2

[[

]]

[[

]]

General Notes

[[

]]

DCD Impact:

No DCD changes will be made in response to this RAI.

Fig. 1:

[[ ]]

[[

]]

Fig. 2:

[[ ]]

[[

]]

Fig. 3:

[[

]]

[[

]]

Fig.4:

[[ ]]

[[

]]

Fig. 5:

[[ ]]

[[

]]

Fig. 6:

[[ ]]

[[

]]

Fig. 7:

[[

]]

]]

Fig. 8:

[[ ]]

[[

]]

Fig. 9:

[[ ]]

[[

]]

Fig. 10:

[[

]]

[[

]]

Fig. 11:

[[

]]

[[

]]

Fig. 12:

[[ ]]

[[

]]

For historical purposes, the original text of RAI 3.6-11 and the GEH response are included. The attachments (if any) are not included from the original response to avoid confusion.

NRC RAI 3.6-11

In the event of a high pressure pipe rupture, the first significant fluid load on surrounding structures would be induced by a blast wave. A spherically expanding blast wave is reasonably approximated to be a short duration transient and analyzed independently of any subsequent jet formation. Since the blast wave is not considered in the ANS 58.2 or the ESBWR DCD for evaluating the dynamic effects associated with the postulated pipe rupture, omission of blast wave considerations is clearly non-conservative. Explain how the effects of blast loads on neighboring SSCs will be accounted for.

GEH Response

Due to the minute difference in time (fraction of seconds), the effects of the spherically forming blast wave will be overpowered by jet impingement force of the emanating fluid from a pipe rupture. The impact of a blast wave on neighboring SSC's is much smaller as the spherical wave expands and the strength reduces significantly in a much short distance than the jet fluid. The density of air is much smaller that the jet. Therefore, the blast loads on neighboring SSCs is negligible as compared to the jet impingement load and it does not become a controlling load.

DCD Impact

No DCD changes will be made in response to this RAI.

NRC RAI 3.6-11 S01

NRC Summary:

Explain how effects of blast waves will be accounted for.

NRC Full Text:

In its response to RAI 3.6-11, GEH stated that the blast loads will be negligible compared to loads caused by jets, citing a lower density of the fluid outside the high energy pipe compared to the jet fluid, and the decay in load amplitude with increasing distance from the break.

Practical experience cited by the international nuclear community, however, clearly shows the strength and damage caused by blast waves (Knowledge Base for Emergency Core Cooling System Recirculation Reliability, February 1996, Issued by the NEA/CSNI, http://www.nea.fr/html/nsd/docs/1995/csni-r1995-11.pdf).

It is unclear why GEH refers to the density of the ambient fluid. It is the pressure ratio between the high energy line and the ambient air that is critical in determining the blast strength. Approximated by the conditions quoted for the high energy piping, an idealized spherical blast wave will be of significant strength near the break. The density, pressure and damaging effect of the ideal blast becomes diminished with radius cubed.

Based on ACRS concerns, and the information in the Knowledge Base for Emergency Core Cooling System Recirculation Reliability, February 1996, Issued by the NEA/CSNI, http://www.nea.fr/html/nsd/docs/1995/csni-r1995-11.pdf, all high pressure and temperature pipes should be considered as sources of blast waves with initial energy and mass roughly equal to the exposed volume from a hypothesized break. The subsequent damage from such waves has been well documented and is not properly accounted for by the isolated analysis of a pure spherically expanding wave. GEH is requested to address these concerns backed by industry operating experience and to provide a rigorous and thorough explanation of their procedures for estimating the effects of blast waves on nearby safety-related SSCs.

GEH Response

[[

]]

[[

]]

Technical Approach

•[[

]]

•[[

]]

[[

]]

Boundary Conditions

[[

]]

[[

]]

Results:

[[

]]

DCD Impact

DCD Tier 2 Subsection 3.6.2.6 will be added in DCD Revision 6 to include a requirement of the blast wave effects evaluation as shown in the attached markup.

Fig. 1:

[[ ]]

[[

]]

Fig. 2:

[[

]]

[[

]]

Fig.3:

[[ ]]

[[

]]

Fig.4:

[[ ]]

[[

]]

For historical purposes, the original text of RAI 3.6-12 and the GEH response are included. The attachments (if any) are not included from the original response to avoid confusion.

NRC RAI 3.6-12

In the characterization of supersonic jets given by ANS 58.2, some physically incorrect assumptions underlie the approximating methodology. The model of the supersonic jet itself is given in Figures C-1 and C-2 of the Standard and contains references to supposedly universal jet characteristics that are not reasonable. A fundamental problem is the assumption that a jet issuing from a high pressure pipe break will always spread with a fixed 45 degree angle up to an asymptotic plane and subsequently spread at a constant 10 degree angle. Each of these characteristics is generally inapplicable and far from universal. Initial jet spreading rate is highly dependent on the ratio of the total conditions of the source flow to the ambient conditions. In reality, subsequent spreading rates depend, at a given axial position,on the ratio of the static pressure in the outermost jet flow region to the ambient static pressure. In the Standard, the asymptotic plane is described as the point at which the jet begins to interact with the surrounding environment. In his critique, Dr. Wallis takes this to mean that the jet is subsonic downstream of the asymptotic plane. In fact, as shown by Wallis and Ransom, supersonic or not, the jet is highly dependent on the conditions in the surrounding medium, and, at a given distance from the issuing break, will spread or contract at a rate depending on the local jet conditions relative to the surrounding fluid pressure.

Supersonic jet behavior can persist over distances from the break far longer than those estimated by the standard, extending the zone of influence of the jet, and the number of SSCs that could be impacted by a supersonic jet. For example, tests in the Seimens-KWU facility in Karlstein, Germany showed that significant damage from steam jets can occur as far as 25 pipe diameters from a rupture (Knowledge Base for Emergency Core Cooling System Recirculation Reliability, February 1996,Issued by the NEA/CSNI, http://www.nea.fr/html/nsd/docs/1995/csni-r1995-11.pdf).

The applicant is requested to:

(a) Explain what analysis and/or testing has been used to substantiate the use of the ANS 58.2 Appendices C and D for defining conservatively which SSCs are in jet paths and the subsequent loading areas on the SSCs.

(b) The applicant states at the bottom of page 3.6-5 that 'impingement force becomes negligible beyond 9.1 meters'; provide the maximum piping and postulated break size dimensions to confirm that 9.1 meters is larger than 25 diameters for all postulated breaks.

GE Response

a) ANS 58.2 is an NRC approved design standard for use in the nuclear industry that has been used by GEH for nuclear plants that are currently operating and/or in the current BWR design. GEH utilized this standard to address the pipe rupture design basis for protection from the potentially adverse effects of a postulated pipe rupture such as, pipe whip, pipe internal loads, jet impingement, room pressurization, environmental conditions and flooding. Specifically, the appendices C and D of the standard were used to evaluate for jet geometry, jet load calculation on target, jet impingement area as a function of distance from the break plane etc.

The GEH methodology used to demonstrate compliance with the standard is demonstrated and can be found in the example calculation "HPCF N16 Nozzle (200 mm) Terminal End Break Jet Impingement Loads". The calculation uses methodology that is representative of that which will be used for the ESBWR. This calculation is a proprietary document that can be made available to the NRC in the GEH offices in Washington, DC or Wilmington, NC.

This calculation illustrates the jet map geometries, various calculation steps in compliance with the methods stipulated in the standard and it computes the pressure distribution as a function of distance from the break location based on a terminal end break at a nozzle. Although no net load on a target was determined, the calculation however provides resulting pressure at various distances from the break. The calculation conservatively determines the equivalent static loads on targets using 2.0 as a Dynamic Load factor (DLF) where applicable. Additionally, the calculation also discusses the determination of the pressure distribution in the radial direction of the jet for targets intercepted in the outer edge of the jet. The net load on a target is calculated using the jet pressure based on the distance of the target from the break and the intercepted area of the jet on the target. A target's shape factor ($K\phi$) may be required to be used as target's potential for changing the momentum of the jet in the net load on the target calculation.

GEH has committed, in the ESBWR DCD, to use approved standard, ANS 58.2, as this standard has been accepted in pipe break evaluations in the nuclear plant design including prior BWR plants by GEH. It may be noted also that GEH has made significant technical contributions to the development of this standard.

It is the conclusion of GEH that these methods substantiate the use of the approved ANS committee standard, ANS 58.2 in the ESBWR pipe rupture design/analysis applications.

b) The ESBWR High Energy piping Inside and Outside Containment are listed below. The table provides a calculation that determines if 25 times the pipe diameter exceeds the 30 ft. distance outside of which the effects of jet impingement is considered negligible as committed in the DCD.

As can be seen in the table below, the main steam piping exceeds the 30ft distance based on 25D calculation. Detailed analysis will be performed for any break location of high and moderate energy piping systems for protection of the safety related components against piping failures inside and outside containment. Additionally, analytical justifications to determine if safety related features require protection against an interacting jet from a pipe break will be provided for targets intercepted by jet outside 25D.

Systems	**Max. Pipe O.D./ Wall thickness (T) Or, Schedule**	**Is 25D greater or less than 30 ft (=9.1 Meter)**
Main Steam	30" Sch.80	25D> 30ft
Feedwater	12"Sch.80	25D<30ft
Control Rod Drive (CRD) System (to and from HCU)	OD =1.25 inch T= 0.183 inch	25D<30ft
Reactor Water Cleanup and Shutdown Cooling System (suction and RPV drain lines)	12 " Sch. 120. RWCU drain line 3" sch. 80	25D<30ft
Isolation Condenser System	14 inch/8 inch Sch.80	25D<30ft
Gravity-Driven Cooling System Injection Lines (from RPV to isolation valves)	6" Sch. 80	25D<30ft
Standby Liquid Control System	2" and 3"sch. 120	25D<30ft

Note: GDCS piping is located inside containment only.

DCD Impact

No DCD changes will be made in response to this RAI.

NRC RAI 3.6-12 S01

NRC Summary:

Address ANS 58.2 jet expansion model inaccuracies.

NRC Full Text:

(a) In its response to part (a) of RAI 3.6-12, GEH does not explain what analysis and/or testing has been used to substantiate using ANS 58.2 Appendices C and D for defining conservatively which SSCs are in jet paths and the subsequent loading on the SSCs. Instead, GEH maintains that it complies with ANS 58.2. GEH has not provided the requested information, and is advised that the ANS 58.2 standard is no longer universally acceptable for modeling jet expansion in nuclear power plants. GEH is encouraged to review the original RAI, along with the criticisms raised by Wallis (Wallis, G., "The ANSI/ANS Standard 58.2-1988: Two-Phase Jet Model," ADAMS ML050830344, 15 Sep 2004) and Ransom (Ransom, V., "COMMENTS ON GSI-191 MODELS FOR DEBRIS GENERATION," ADAMS ML050830341, 15 Sep 2004) and prepare a thorough response.

(b) In its response to part (b) of RAI 3.6-12, GEH provides a table of maximum pipin(sic) and postulated break dimensions and compares 25 diameters to its maximum impingement distance of 9.1 meters. 25 diameter distances from all all (sic) piping, except for the Main Steam Lines (MSLs), are less than 9.1 meters. However, 25 diameters from the MSLs is 19.1 meters, 10 meters more than GEH's maximum impingement distance of 9.1 meters. GEH states that "analytical justifications to determine if safety related features require protection against an interacting jet from a pipe break will be provided for targets intercepted by jet outside 25D." However, GEH has not added this commitment the DCD. Since the 25 diameter distance from the Main Steam Lines is 19.1 m, 10 m more than GEH's maximum jet impingement distance of 9.1 m, GEH is requested to revise the DCD to state that the loads on any SSCs within 19.1 m of postulated ruptures of the MSLs will be assessed, along with the structural integrity of the SSCs.

GEH Response

(a) The response to RAI 3.6-6 S02 provides all break locations for inside and outside of the containment. The response also includes the jet analysis methods to be used associated with each high energy line pipe break. Where applicable, the jet impingement effects from a pipe break will be evaluated by performing a nonlinear transient CFD analysis and jet load on targets will be determined. The fluid properties for each break inside and outside containment are discussed in responses to RAI 3.6-13 S01. The ANSYS CFD analysis computer program that performs nonlinear transient analysis of jet effects will accurately capture the shock wave effects, jet reflection, feedback amplifications, and jet unsteadiness characteristics. The jet load pressure on an SSC is determined by this analysis method and the resolution of the jet impact will be addressed for the interaction to the SSCs.

In certain cases a detailed jet analysis may not be necessary if it can be established that a load on a target has been conservatively determined from a pipe break and the magnitude of the jet loads for the same target from other breaks will not exceed the calculated maximum load.

Additionally, based on engineering judgment, a simplified approach (as discussed in part C of RAI 3.6-6 S02) rather than a detailed jet analysis is acceptable to determine the jet thrust force. Also, in some cases a similarity approach can be used on the basis of the similarity from the standpoint of piping geometry and other break conditions such as the pipe size, fluid energy reservoir upstream of the break etc., and in such cases, the results from a detailed pipe break evaluation may be directly applicable to the other similar pipe breaks.

Based on the methods that are discussed above and all pipe breaks with resolutions as illustrated in the response to RAI 3.6-6 S02, the ANS 58.2 appendices C and D methods will not be used in the ESBWR pipe break jet evaluations.

(b) DCD will be revised to include an exception to the 9.1 meter rule. Instead, 19.1 meters will be used as the evaluation zone and structural interaction determination for the MS line breaks. The jet effects will be analyzed based on the CFD analysis method (see response to RAI 3.6-6 S02).

DCD Impact

In reference to the response to item (b) above, DCD Tier 2, Section 3.6.1.3 will be revised in DCD Revision 6 to include an exception to the rule of 9.1 meters (30 ft.) for the main steam line breaks. For MS breaks, 19.1 meters (63 ft.) will be used for jet impingement effects.

For historical purposes, the original text of RAI 3.6-13 and the GEH response are included. The attachments (if any) are not included from the original response to avoid confusion.

NRC RAI 3.6-13

The ANS 58.2 standard formulas for the spatial distribution of pressure through a jet cross-section are incorrect, as pointed out by Wallis and Ransom. In some cases,the standard's assumption that the pressure within a jet cross section is maximum at the jet centerline is correct (near the break, for instance), but far from the break, the pressure variation is quite different, often peaking near the outer edges of the jet. Applying the standard's formulas could lead to non-conservative pressures away from the jet centerline.

The applicant states the following on page 3.6-18 of Section 3.6.2 of ESBWR DCD Tier 2: "The jet impingement force is uniformly distributed across the crosssectional area of the jet and only the portion intercepted by the target is considered". The applicant also states that ANS 58.2 Appendix D is used, which defines variable (not uniform) pressures over the cross-section of an expanding jet (see comments above regarding the inaccuracies of ANS Appendix D). The standard does specify a uniform pressure over the cross-section of a non-expanding jet, so it appears that the applicant is mixing the methods of the standard, combining the shape of an expanding jet with the uniform pressure distribution of a non-expanding jet.

The applicant is requested to:

(a) Clarify which approach (variable pressure over an expanding jet cross-section as defined in Appendix D of ANS 58.2, or a uniform pressure distribution assumed in DCD) will be used to specify pressure distribution over an expanding jet cross section. In either case, the applicant should explain what analysis and/or testing has been used to substantiate use of the ANS 58.2 Appendix D and/or the formulas in DCD Tier 2 for defining conservatively the net jet impingement loading on SSCs in light of the information presented by Ransom and Wallis (ADAMS ML050830344,ADAMS ML050830341), which challenges the accuracy of the pressure distribution models presented in ANS 58.2.

(b) Submit a table of all postulated break types, along with the properties of the fluid internal and external to the ruptured pipe. The table should specify what type of jet the applicant assumes will emanate from each pipe break - incompressible nonexpanding jet, or compressible supersonic expanding jet - along with how impingement forces will be calculated for each jet. Specific examples of jet impingement loading calculations made using the ANS 58.2 standard and/or the methods in DCD Tier 2 for the postulated piping breaks in an ESBWR should be given, along with proof that the calculations lead to conservative impingement loads in spite of the cited inaccuracies and omissions in the ANS 58.2 models pointed out by Ransom and Wal

GEH Response

NRC item a) has questions in two parts:

Part i) *Clarify which approach (variable pressure over an expanding jet cross-section as defined in Appendix D of ANS 58.2, or a uniform pressure distribution assumed in DCD) will be used to specify pressure distribution over an expanding jet cross section*

As stated in ANS Standard 58.2, the pressure distribution on a target may be derived using variable as well as uniform distribution methods depending on the fluid and jet characteristics at the exit of the break. DCD Tier 2,Subsection 3.6.2.3.1 will be revised to identify that Appendix D methods will be used for the pressure distribution evaluations.

Part ii) *In either case, the applicant should explain what analysis and/or testing has been used to substantiate use of the ANS 58.2 Appendix D and/or the formulas in DCD Tier 2 for defining conservatively the net jet impingement loading on SSCs in light of the information presented by Ransom and Wallis (ADAMS ML050830344, ADAMS ML050830341), which challenges the accuracy of the pressure distribution models presented in ANS 58.2.*

GEH has committed, in the ESBWR DCD, to use of the approved standard ANS 58.2, as this standard has been accepted in pipe break evaluations in the nuclear plant design including prior BWR plant pipe rupture evaluations performed by GEH. It may be noted that GEH has made significant technical contributions to the development of this standard.

The GEH methodology used to demonstrate compliance with the standard is demonstrated and can be found in the example calculation "HPCF N16 Nozzle (200 mm) Terminal End Break Jet Impingement Loads". The calculation uses methodology that is representative of that which will be used for the ESBWR. This calculation is a proprietary document that can be made available to the NRC in the GEH offices in Washington, DC or Wilmington, NC.

This calculation illustrates the jet map geometries, various calculation steps in compliance with the methods stipulated in the standard and computes the pressure distribution as a function of distance from the break location based on a terminal end break at a nozzle. Although no net load on a target was determined, the calculation however provides resulting pressure at various distances from the break. The calculation conservatively determines the equivalent static loads on targets using 2.0 as a Dynamic Load factor (DLF) where applicable. Additionally, the calculation also discusses the determination of the pressure distribution in the radial direction of the jet for targets intercepted in the outer edge of the jet. The net load on a target is calculated using the jet pressure based on the distance of the target from the break and the intercepted area of the jet on the target. A target's shape factor ($K\phi$) may be required to be used as target's potential for changing the momentum of the jet in the net load on the target calculation.

In conclusion, the use of ANS Standard and design bases as described in the DCD Tier 2 Chapter 3.6 will be conservative and adequately address the protection against pipe failures for the ESBWR pipe rupture design/analysis.

(b) All ESBWR piping will be designed to minimize the stresses and fatigue usage factors such that piping intermediate break locations are avoided. Therefore, all postulated pipe break locations are the terminal end breaks at RPV and/or at the equipment nozzles. Conservatively, double-ended break is assumed for all breaks. Fluid pressure and temperature for an assumed break are the same as the applicable nozzles. For low temperature sub-cooled fluid condition, a non-expanding jet will be assumed otherwise an expanding jet will be used for the jet impingement. Based on the results from the pipe rupture analysis, the necessary protective devices will be designed and installed to mitigate the effects of the pipe break postulations in the high and moderate energy ESBWR piping systems.

DCD Impact

DCD Tier 2, Subsection 3.6.2.3.1 will be revised as noted in the attached markup.

NRC RAI 3.6-13 S01

NRC Summary:

Address ANS 58.2 and DCD Tier 2 jet pressure distribution inaccuracies and inconsistencies.

NRC Full Text:

(a) GEH clarifies in its response to part (a) of RAI 3.6-13 that it will use Appendix D of ANS 58.2 methods to compute pressure distributions on a target, and that DCD Tier 2, Subsection 3.6.2.3 has been modified accordingly. However, GEH has not addressed the second question in part (a), which is to explain what analysis and/or testing has been used to substantiate the use of Appendix D of ANS 58.2 in light of ACRS criticisms. Instead GEH states that it complies with ANS 58.2. It should be noted that the ANS 58.2 standard, including Appendix D, is no longer universally acceptable for specifying jet pressure distributions over SSCs in nuclear power plants. In particular, the effects of compressibility and unsteadiness are neglected. GEH is encouraged to review the original RAI, along with the criticisms raised by Wallis (Wallis, G., "The ANSI/ANS Standard 58.2-1988: Two-Phase Jet Model," ADAMS ML050830344, 15 Sep 2004) and Ransom (Ransom, V., "COMMENTS ON GSI-191 MODELS FOR DEBRIS GENERATION," ADAMS ML050830341, 15 Sep 2004) and prepare a thorough response.

(b) GEH has provided only general, incomplete and vague information in response to RAI 3.6-13(b). GEH does state, however, that the pipes have been designed such that breaks may only occur at the terminal ends. The original RAI requested the applicant to submit a table of all postulated break types, along with the properties of the fluid internal and external to the ruptured pipe. The table should specify what type of jet the applicant assumes will emanate from each pipe break? incompressible nonexpanding jet, or compressible supersonic expanding jet?along with how impingement forces will be calculated for each jet. Specific examples of jet impingement loading calculations made using the ANS 58.2 standard and/or the methods in DCD Tier 2 for the postulated piping breaks in an ESBWR should be given, along with proof that the calculations lead to conservative impingement loads in spite of the cited inaccuracies and omissions in the ANS 58.2 models pointed out by Ransom and Wallis. GEH is requested to provide a detailed and thorough response to the original RAI 3.6 -13 (b).

GEH Response:

(a) Refer to the response and tables 1 and 2 in RAI 3.6-6 S02 for detailed analysis approach for each break with justifications.

(b) The ESBWR high energy line parameters for fluid properties, environmental conditions, and the jet types associated with breaks are provided below. DCD Tier 2, subsection 3.6, Tables 3.6-3 and 3.6-4 identify the high energy piping inside and outside containment.

The following tables provide pipe break locations, environmental conditions, and break conditions for piping inside and outside containment.

[[

]]

[[

]]

[[

]]

[[

]]

DCD Impact

No DCD changes will be made in response to this RAI.

For historical purposes, the original text of RAI 3.6-14 and the GEH response are included. The attachments (if any) are not included from the original response to avoid confusion.

NRC RAI 3.6-14

On page 3.6-18, the applicant states that "The total impingement force acting on any cross-sectional area of the jet is time and distance invariant with a total magnitude equivalent to the steady-state fluid blowdown force given in Subsection 3.6.2.2 and with jet characteristics shown in Figure 3.6-1". While this may be true for some subsonic non-expanding jets, it is certainly not true for supersonic expanding jets, particularly those impinging on nearby structures. The applicant is requested to examine the following reference, "Knowledge Base for Emergency Core Cooling System Recirculation Reliability, February 1996, Issued by the NEA/CSNI," (http://www.nea.fr/html/nsd/docs/1995/csni-r1995-11.pdf), which states that tests in Germany's Heissdampfreactor (HDR) showed high dynamic (oscillating) loads in the immediate vicinity of breaks. The applicant provides additional criteria and procedures for jet loading evaluations in Appendix 3J.5 of the DCD. The applicant explains that the dynamic component of jet loading is considered independently from the static component, and that when static analysis methods are used to assess dynamic jet loads, the results are to be multiplied by a factor of two. However, in Section 3.6.2 of the DCD/Tier 2, Rev. 01, the applicant assumes that all jet loads are time invariant.

Free jets are notoriously unsteady and, in the case of supersonic jets, such strong unsteadiness will tend to propagate in the shear layer and induce unsteady (timevarying oscillatory) loads on obstacles in the flow path. Pressures and densities vary nonmonotonically with distance along the axis of a typical supersonic jet and this in turn feeds and interacts with shear layer unsteadiness. In addition, for a typical supersonic jet, interaction with obstructions will lead to backward-propagating transient shock and expansion waves that will cause further unsteadiness in downstream shear layers.

In some cases, synchronization of the transient waves with the shear layer vortices emanating from the jet break can lead to significant amplification of the jet pressures and forces (a form of resonance) that is not considered in the ANS 58.2 standard and DCD Tier 2. Should the dynamic response of the neighboring structure also synchronize with the jet loading time scales, further amplification of the loading can occur, including that at the source of the jet. These feedback phenomena are wellknown to those in the aerospace industry who work with aircraft that use jets to lift off and land vertically [see, for example Ho, C.M., and Nosseir, N.S., "Dynamics of an impinging jet. Part 1. The feedback phenomenon," Journal of Fluid Mechanics,Vol. 105, pp. 119-142, 1981]. Some general observations by past investigators are that strong discrete frequency loads are observed when the impingement surface is within 10 diameters of the jet opening, and that when resonance within the jet occurs, significant amplification of impingement loads can result (Ho and Nosseir show a factor of 2-3 increase in pressure fluctuations at the frequency of the resonance).

The applicant is requested to:

(a) Provide information that establishes that the applicant's interpretation of the jet impingement force as static is conservative.

(b) Explain whether any postulated pipe break locations are within 10 diameters of a neighboring SSC (or barrier/shield), and if so, how jet feedback/resonance and resulting dynamic load amplification are accounted for.

(c) Clarify whether dynamic jet loads are to be considered, and if so, using what methods. Also, should the dynamic loading include strong excitation at discrete frequencies corresponding to resonance frequencies of the SSC impinged upon,provide the basis for assuming a static analysis with a dynamic load factor of two is conservative.

GEH Response

a) When the steady state thrust is greater than the initial thrust, the time dependent thrust force may be assumed to rise to the steady state thrust force and remain constant with time. Using an appropriate thrust coefficient (C_T) based on the fluid properties, the static jet force can be calculated as $F_{jet} = C_T P A$. Where, P = Exit pressure of the broken pipe, and A= Cross sectional area of the broken pipe end. This static load is conservative since f L/D is zero or very small,

   Where,

   f = Pipe Friction factor

   L/D = Pipe Length to Diameter Ratio

b) As part of the detail design, the pipe rupture evaluation will address the exact location of the potential targets such as, SSCs (or barrier/shield), and provide resolutions in mitigating the consequence of pipe rupture impact.

   For feedback/resonance, the resulting dynamic amplification will get automatically accounted for in when blowdown time-history dynamic response evaluations for the pipe rupture loads on the impacted component/structure are performed. Also, instead of a dynamic analysis, an equivalent static analysis can be performed with the use of a dynamic load factor as follows:

   $F_S = DLF\ (F_{imp\ max})$

   Where,

   F_S = Equivalent static impingement force

   DLF = Dynamic load factor

   $F_{imp\ max}$ = Maximum value of the jet impingement force

The impingement force may conservatively be assumed to occur instantaneously and a DLF = 2.0 is used. A separate value for DLF may be analytically established based on DLF = *dynamic deflection/ static deflection* of the object being impinged upon.

c) This question has two parts:

i. *Clarify whether dynamic jet loads are to be considered, and if so, using what methods.*

ANS 58.2 methods will be used to determine the blowdown loads.

ii. *Also, should the dynamic loading include strong excitation at discrete frequencies corresponding to resonance frequencies of the SSC impinged upon, provide the basis for assuming a static analysis with a dynamic load factor of two is conservative.*

Refer response to the item b) above for consideration of feedback resonance in design.

As stated in ANS 58.2 section 7.3, an equivalent static analysis, a dynamic load factor (DLF) of 2 is conservative. This is because ANS 58.2 assumes the jet impingement force to have 0.001 second rise time and reaches constant value. The force has no discrete frequencies corresponding to resonance frequencies of the SSC being impinged upon. Figure a) below shows the "Maximum response of one-degree elastic system (undamped) subjected to rectangular and triangular pulse having zero rise time " from "Introduction to structural dynamic" by John M Biggs. The maximum DLF is 2.0. If the rise time is considered, the DLF will be less than 2.0. For multiple degree system subject to jet impingement load, the maximum dynamic load factor (DLF) of 2 is also applicable.

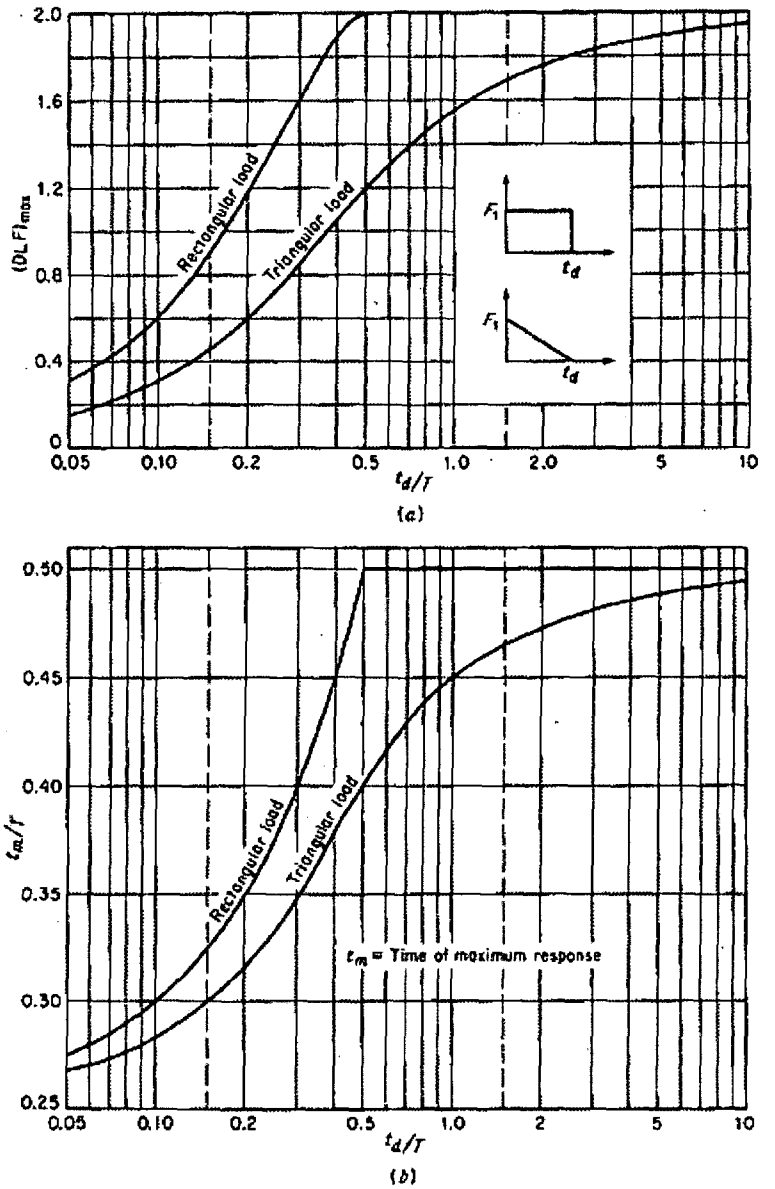

FIGURE 2.7 Maximum response of one-degree elastic systems (undamped) subjected to rectangular and triangular load pulses having zero rise time. (*U.S. Army Corps of Engineers.*[10])

DCD Impact

No DCD changes will be made in response to this RAI.

NRC RAI 3.6-14 S01

NRC Summary:

Justify neglecting jet dynamic loading and structural dynamic response, and neglecting feedback amplification of dynamic jet loads.

NRC Full Text:

(a) In its response to part (a) of RAI 3.6-14, GEH describes an approach for obtaining the load due to jet impingement. In the GEH approach, it is assumed that there is a thrust coefficient that may be used to obtain a conservative, but static, load applied by the jet. Thus an unsteady, nonuniform load is replaced, for analysis, with a uniform, constant load. It is unclear that this is consistent with a compressible flow analysis. It has been documented, in the comments of Wallis and Ransom and the Knowledge Base for Emergency Core Cooling System Recirculation Reliability (February 1996, Issued by the NEA/CSNI, http://www.nea.fr/html/nsd/docs/1995/csni-r1995-11.pdf) that such high-energy free expanding jets will generally contain a complex of oblique shock and expansion waves and an unsteady shear layer. There will be significant

unsteadiness and nonuniformity. GEH is requested to provide a response that clearly demonstrates a conservative approach for what is properly considered as a compressible, turbulent, unsteady flow.

(b) GEH states in its response to part (b) of RAI 3.6-14 that dynamic amplification will be automatically accounted for in when blow down time history-dynamic response evaluations for the pipe rupture loads on the impacted component/structure are performed. However, GEH does not provide any details on its analysis approach. GEH also, as in its response to RAI 3.6-6 S01, provides a conflicting static analysis approach using a DLF of 2.0. It is unclear which approach it plan to use. GEH is requested to provide the additional information to establish that it is conservative to use DLF of 2, if the static analysis approach is used. In addition, GEH is requested to explain how its nonlinear time-history analysis addresses feedback and resonance including all validation exercises, and bias errors/uncertainties associated with their analysis approach.

(c) GEH ignores dynamic jet loads in its response to part (c) of RAI 3.6-14, relying on the assumed 0.001 second rise time in the ANS 58.2 standard as the only time-dependent component of their jet loads. However, much of the original RAI 3.6-14 provides citations to existing literature which clearly substantiate the presence of dynamic effects in actual jets. GEH is advised that the ANS 58.2 standard is no longer universally acceptable for specifying jet loads over SSCs in nuclear power plants, and that dynamic effects beyond those due to the initial transient assumed in ANS 58.2 must now be considered in the DCD. GEH is requested to review the original RAI and provide a detailed and thorough response concerning how the dynamic jet loads are considered and provide the basis for assuming a static analysis with a dynamic load factor of two is conservative.

GEH Response

(a) See response to RAI 3.6-6 S02. This RAI response provides analysis approach for each pipe break case and justification for the method to be used to determine the jet effects.

(b) Analysis methodology for all high energy line break is identified in the response to part (a).

CFD method will be used that evaluates the non-linear time history condition. The CFD will handle the interaction between the shock waves and the surrounding objects by solving the transient Navier-Stoke equations for flow field and hence, the nonlinearity, feedback amplification and resonance effects are captured in the analysis.

For DLF = 2.0, see response to RAI 3.6-6 S02.

(c) The pipe break analysis methodologies for each break have been identified in RAI 3.6-6 S02. As stated above the computational fluid dynamics program CFX will be used where justified and applicable to predict the dynamic loads due to the jet force.

A detailed evaluation was recently performed for a typical BWR4 "Steam Dryer Acoustic Load Predictions in the Main Steam Line Break Event" (presented by Jin Yan et. el of GEH in the 16th International Conference on Nuclear Engineering, May 11-15, 2008 in Orlando, Fl., USA). This report (attached) describes a complete evaluation technique for the MSLB pipe break using the CFX program.

The report indicates that a transient simulation time step of 4e-6 second was carried out.

The conclusion of the transient analysis report stated the following:

"Transient CFD simulations of the Main Steam Line break event were completed on a half model of a BWR4 RPV. A single shock tube simulation was carried out to validate the accuracy of the CFD approach. A high fidelity mesh with all hexahedral cells was generated to minimize the numerical diffusion. The shock wave and the expansion wave development have been observed in the results. The maximum differential pressure across the dryer hood and the cover plate are reported. The differential pressure across the cover plate of the dryer is higher than that on the dryer hood. The reflection of the wave between the dryer hood and the vessel wall is captured by the CFD solution. Compared to the traditional methods, CFD can not only predict the maximum differential pressure, but also the location of where the maximum differential pressure is on the structure."

DCD Impact

No DCD changes will be made in response to this RAI.

For historical purposes, the original text of RAI 3.6-15 and the GEH response are included. The attachments (if any) are not included from the original response to avoid confusion.

NRC RAI 3.6-15

The applicant defines the limiting temperature (93.3 C) and pressure (1.9 MPaG) which separate the definitions of high energy and moderate energy fluid systems. However, the staff could not locate readily the maximum temperature and pressure in the high energy systems. Many of the staff's RAIs are related to potential errors in modeling the many types of jets which could emanate from different piping breaks; however some of the RAIs may refer to jet types that are not applicable to the ESBWR design. So that the staff may better understand the types of jets and blast waves which might emanate from the postulated breaks in ESBWR, clarify maximum expected high energy line temperature, pressure, and pipe diameter.

GEH Response

The ESBWR high energy line parameters are provided below (Ref. DCD Tier 2, subsection 3.6, Tables 3.6-3 (High Energy Piping Inside Containment) and 3.6-4 (High Energy Piping Outside Containment) of DCD Tier 2, Rev.3.

High Energy Piping Inside and Outside Containment

Systems	Maximum Temperature (°F)	Maximum Pressure (MPa/Psig)	Max. Pipe O.D./ Wall thickness (T) Or, Schedule
Main Steam	575	8.62 MPa (1250 psig)	OD =28 inch T = 1.45"
Feedwater	420	7.31 MPa (1060 psig)	12" Sch.80
Control Rod Drive (CRD) System (to and from HCU)	150	23.54 MPa (3414 psig)	1.25 inch T= 0.183 inch
Reactor Water Cleanup and Shutdown Cooling System (suction and RPV drain lines)	575	9.48 MPa (1374 psig)	12 " Sch. 120. RWCU drain line 3" Sch. 80
Isolation Condenser System	598	10.34 MPa (1500 psig)	14 inch/8 inch sch.80
Gravity-Driven Cooling System Injection Lines (from RPV to isolation valves)	572	8.62 MPa (1250 psig)	6" Sch. 80
Standby Liquid Control System	533	15.20 MPa (2204 psig)	2" and 3"sch. 120

Notes:
1. GDCS piping is located inside containment only.

2. The maximum temperature and pressure values used herein for CRD piping are from GE's Lungmen Nuclear Power Project (Taiwan Power Company)
3. Systems pressure and/or temperature are estimated values only. These values may differ slightly or coincide when final design is complete.

DCD Impact

No DCD changes will be made in response to this RAI.

NRC RAI 3.6-15 S01

NRC Summary:

Clarify maximum expected high energy line temperature, pressure, and pipe diameter.

NRC Full Text:

In its response to RAI 3.6-15, GEH provided the table requested. However, to allow the staff to review GEH's future responses to other RAIs associated with jet loads and blast loads on nearby safety-related SSCs, the conditions of regions outside the high energy piping are required. GEH is requested to add the temperature and pressure of the regions outside the high energy piping systems to the table provided in its initial RAI response. This information will also be required for GEH's response to the follow-up RAI 3.6-13(b) S01

GEH Response

ESBWR high energy pipes are located inside the containment, in the reactor building and turbine building. The temperature and pressure for the regions outside of the high energy piping are shown in the tables provided in the response to RAI 3.6-13 S01. This information was obtained from tables 3H-2 and 3H-3 in Appendix H of DCD Tier 2 for inside and outside the containment respectively. The ambient condition pressure and temperature for turbine building are obtained from DCD Tier 2, Table 9.4-15 of chapter 9.

DCD Impact

No DCD changes will be made in response to this RAI.

For historical purposes, the original text of RAI 3.6-16 and the GEH response are included. The attachments (if any) are not included from the original response to avoid confusion.

NRC RAI 3.6-16

The applicant states at the bottom of page 3.6-17 of Section 3.6.2 of ESBWR DCD Tier 2 that 'reflected jets are considered only when there is an obvious reflecting surface (such as a flat plate)'. Explain quantitatively how the reflections will be considered.

GEH Response

Conservatively, reflective force of the jet may be assumed equal to the jet striking force based on the jet pressure on the plate neglecting the friction and energy loss of the striking jet upon hitting the plate. The shape factor may be applicable based on the orientation of the plate in the jet stream.

DCD Impact

No DCD changes will be made in response to this RAI.

NRC RAI 3.6-16 S01

NRC Summary: Explain how jet reflections will be assessed.

NRC Full Text:

In its response to RAI 3.6-16, GEH states that the reflective force of the jet may be conservatively addressed using a shape factor and the assumed momentum of the jet. GEH has not discussed how they address the unsteadiness, compressibility, and coupled structural interaction with the jet. GEH is requested to modify DCD to clearly delineate how candidate reflecting surfaces are chosen and how this analysis addresses the unsteadiness, compressibility, and coupled potentially resonant, structural interaction with the jet.

GEH is also requested to summarize its quantitative approach for modeling reflections in a revised DCD.

GEH Response

The response to this RAI question is provided in two segments.

[[

]]

[[

]]

[[

]]

[[

]]

[[

]]

[[

]]

Part 2: Resonance

a.) For inside containment terminal end breaks (Table 1 above) the following interactions will result:

GDCS pool for main steam break

RPV and RSW for breaks in the annulus region between the RPV and RSW

- Concrete floor mat, and RPV pedestal for the terminal end breaks at the RWCU drain nozzle.

Main steam line break will be analyzed by CFD analysis approach as described in RAI response to RAI 3.6-6 S02. The analysis can provide the force time history of the interacting jet at the target location. A dynamic analysis of the GDCS pool structure with appropriate boundary condition and with the time history as the input load will be performed to obtain the responses in terms of forces and moments for GDCS structural integrity evaluations.

The RPV and RSW are identified as reactor building internal structures. These structures are designed to withstand the worst load impact due to static and various dynamic loads and combinations of these loads including the effects from the jet load. A structural evaluation of the ESBWR reactor building and internal structure has been performed using the NASTRAN finite element program. The ESBWR design details of Reinforced Concrete Containment Vessel (RCCV) and other internal structures are found in DCD Tier 2, section 3.8 and appendices 3F, and 3G.

In addition to the above, the ESBWR pipe rupture evaluations will also adequately address the containment structural integrity resulting from any pipe break inside the containment.

b) For outside containment terminal end breaks, the breaks are located in a separate enclosures or rooms other than the main steam terminal end breaks at header near the turbine stop valve in the turbine building. Currently, there are no safety related equipment or component inside these rooms. As applicable, the rupture restraint will be designed for these piping to restrict the pipe whip and uncontrolled jet impact. Breaks at the header for main steam piping will be analyzed by CFD program. Potential safety-related targets (if any) would be identified, analyzed and documented.

It may be noted that the use of pipe rupture support justified by design and analysis on piping system for inside and outside containment will prevent or minimize the development of a full-blown jet impingement impact.

DCD Impact

DCD Tier 2, Subsection 3.6.2.3.1 will be revised in DCD Revision 6 to include additional method for analyzing jet impingement from a pipe break as shown in the attached markup.

For historical purposes, the original text of RAI 3.6-17 and the GEH response are included. The attachments (if any) are not included from the original response to avoid confusion.

NRC RAI 3.6-17

The applicant states that in some cases, barriers, shields, and enclosures around high-energy lines will be specified (page 3.6-6). These nearby surfaces can induce feedback and resonance within jets, potentially destroying the barrier, shield, or enclosure. Explain how the barriers, shields, and enclosures will be designed so that they will not be damaged or destroyed by dynamic jet resonant loading.

GEH Response

ANS 58.2 Appendices C and D will be used to determine the jet impingement load. Structures such as, barriers, shield, or enclosures are conservatively designed in order to withstand a large load such as jet impingement loads.

As stated in ANS 58.2 section 7.3, either a dynamic analysis or an equivalent static analysis may be performed for jet impingement loads for evaluations on targets and/or barriers. In absence of a dynamic analysis, an equivalent static analysis may be used where a dynamic load factor (DLF) of 2 may be applied to determine the jet load. A time history analysis or equivalent static load application as input will be adequate in determining the structural response for barriers, shields, and enclosures.

Barriers or shields that are identified as necessary by the High Energy Line Separation Analysis (HELSA) evaluation (i.e., based on no specific break locations) are designed for worst-case loads. The closest high-energy pipe location and resultant loads are used to size the barriers.

DCD Impact

No DCD changes will be made in response to this RAI.

NRC RAI 3.6-17 S01

NRC Summary:

Explain barrier, shield, and enclosure design considerations related to jet resonance effects.

NRC Full Text:

In its response to RAI 3.6-17, GEH explains that it plan to use ANS 58.2 to design barriers, shields, and enclosures around high energy lines. An equivalent static analysis with DLF of 2 will be used. GEH does not address the possibility of dynamic jet resonant loading in its response. That is unacceptable to the staff. GEH is advised that the ANS 58.2 standard is no longer universally acceptable for specifying jet loads over barriers, shields, and enclosures in nuclear power plants, and that, dynamic effects beyond those due to the initial transient assumed in ANS 58.2 must now be considered in the DCD. GEH is requested to consider realistic jet loads which include dynamic effects and possible resonant amplification in its response to this RAI.

GEH Response

Pipe break locations and the applicable analysis methods associated with each break are provided in response to RAI 3.6-6 S02. As applicable, for cases where a dynamic analysis is performed, the time history analysis of jet blowdown to SSCs is capable of capturing the effects of the possible resonant amplification.

DCD Impact;

1. DCD Tier 2, Subsection 3.6.2.3.1 will be revised in DCD Revision 6 to include a paragraph on the dynamic analysis technique of structure for jet impingement interaction load based on the force time history as shown in the attached markup.

2. DCD Tier 2, Appendix 3D will be revised in DCD Revision 6 to include RELAP5 and ANSYS CFX computer software programs as noted in the attached markup.

MFN 08-968

Enclosure 3

Affidavit

GE-Hitachi Nuclear Energy Americas LLC

AFFIDAVIT

I, David H. Hinds, state as follows:

(1) I am the Manager, New Units Engineering, GE Hitachi Nuclear Energy ("GEH"), have been delegated the function of reviewing the information described in paragraph (2) which is sought to be withheld, and have been authorized to apply for its withholding.

(2) The information sought to be withheld is contained in Enclosure 1 of GEH letter MFN 08-968, Mr. Richard E. Kingston to U.S. Nuclear Regulatory Commission, entitled *Response to Portion of NRC RAI Letter No. 185 Related to ESBWR Design Certification Application – DCD Tier 2 Section 3.6 – Protection Against Dynamic Effects Associated With The Postulated Rupture Of Piping; RAI Numbers 3.6-6 S02, 3.6-11 S01, 3.6-12 S01, 3.6-13 S01, 3.6-14 S01, 3.6-15 S01, 3.6-16 S01, 3.6-17 S01,* dated December 30, 2008. The GEH proprietary information in Enclosure 1, which is entitled *Response to Portion of NRC RAI Letter No. 185 Related to ESBWR Design Certification Application – DCD Tier 2 Section 3.6 – Protection Against Dynamic Effects Associated With The Postulated Rupture Of Piping; RAI Numbers 3.6-6 S02, 3.6-11 S01, 3.6-12 S01, 3.6-13 S01, 3.6-14 S01, 3.6-15 S01, 3.6-16 S01 and 3.6-17 S01 - Proprietary Version,* is delineated by a [[dotted underline inside double square brackets.{3}]]. Figures and large equation objects are identified with double square brackets before and after the object. In each case, the superscript notation {3} refers to Paragraph (3) of this affidavit, which provides the basis for the proprietary determination. A non-proprietary version of this information is provided in Enclosure 2, *Response to Portion of NRC RAI Letter No. 185 Related to ESBWR Design Certification Application – DCD Tier 2 Section 3.6 – Protection Against Dynamic Effects Associated With The Postulated Rupture Of Piping; RAI Numbers 3.6-6 S02, 3.6-11 S01, 3.6-12 S01, 3.6-13 S01, 3.6-14 S01, 3.6-15 S01, 3.6-16 S01, 3.6-17 S01 - Public Version.*

(3) In making this application for withholding of proprietary information of which it is the owner, GEH relies upon the exemption from disclosure set forth in the Freedom of Information Act ("FOIA"), 5 USC Sec. 552(b)(4), and the Trade Secrets Act, 18 USC Sec. 1905, and NRC regulations 10 CFR 9.17(a)(4), and 2.390(a)(4) for "trade secrets" (Exemption 4). The material for which exemption from disclosure is here sought also qualify under the narrower definition of "trade secret," within the meanings assigned to those terms for purposes of FOIA Exemption 4 in, respectively, Critical Mass Energy Project v. Nuclear Regulatory Commission, 975F2d871 (DC Cir. 1992), and Public Citizen Health Research Group v. FDA, 704F2d1280 (DC Cir. 1983).

(4) Some examples of categories of information which fit into the definition of proprietary information are:

a. Information that discloses a process, method, or apparatus, including supporting data and analyses, where prevention of its use by GEH competitors without license from GEH constitutes a competitive economic advantage over other companies;

b. Information which, if used by a competitor, would reduce his expenditure of resources or improve his competitive position in the design, manufacture, shipment, installation, assurance of quality, or licensing of a similar product;
c. Information which reveals aspects of past, present, or future GEH customer-funded development plans and programs, resulting in potential products to GEH;
d. Information which discloses patentable subject matter for which it may be desirable to obtain patent protection.

The information sought to be withheld is considered to be proprietary for the reasons set forth in paragraphs (4)a., and (4)b, above.

(5) To address 10 CFR 2.390(b)(4), the information sought to be withheld is being submitted to NRC in confidence. The information is of a sort customarily held in confidence by GEH, and is in fact so held. The information sought to be withheld has, to the best of my knowledge and belief, consistently been held in confidence by GEH, no public disclosure has been made, and it is not available in public sources. All disclosures to third parties including any required transmittals to NRC, have been made, or must be made, pursuant to regulatory provisions or proprietary agreements which provide for maintenance of the information in confidence. Its initial designation as proprietary information, and the subsequent steps taken to prevent its unauthorized disclosure, are as set forth in paragraphs (6) and (7) following.

(6) Initial approval of proprietary treatment of a document is made by the manager of the originating component, the person most likely to be acquainted with the value and sensitivity of the information in relation to industry knowledge, or subject to the terms under which it was licensed to GEH. Access to such documents within GEH is limited on a "need to know" basis.

(7) The procedure for approval of external release of such a document typically requires review by the staff manager, project manager, principal scientist or other equivalent authority, by the manager of the cognizant marketing function (or his delegate), and by the Legal Operation, for technical content, competitive effect, and determination of the accuracy of the proprietary designation. Disclosures outside GEH are limited to regulatory bodies, customers, and potential customers, and their agents, suppliers, and licensees, and others with a legitimate need for the information, and then only in accordance with appropriate regulatory provisions or proprietary agreements.

(8) The information identified in paragraph (2), above, is classified as proprietary because it identifies detailed GE ESBWR design information. GE utilized prior design information and experience from its fleet with significant resource allocation in developing the system over several years at a substantial cost.

The development of the evaluation process along with the interpretation and application of the analytical results is derived from the extensive experience database that constitutes a major GEH asset.

(9) Public disclosure of the information sought to be withheld is likely to cause substantial harm to GEH's competitive position and foreclose or reduce the availability of profit-making opportunities. The information is part of GEH's comprehensive BWR safety and technology base, and its commercial value extends beyond the original development cost. The value of the technology base goes beyond the extensive physical database and analytical methodology and includes development of the expertise to determine and apply the appropriate evaluation process. In addition, the technology base includes the value derived from providing analyses done with NRC-approved methods.

The research, development, engineering, analytical and NRC review costs comprise a substantial investment of time and money by GEH.

The precise value of the expertise to devise an evaluation process and apply the correct analytical methodology is difficult to quantify, but it clearly is substantial.

GEH's competitive advantage will be lost if its competitors are able to use the results of the GEH experience to normalize or verify their own process or if they are able to claim an equivalent understanding by demonstrating that they can arrive at the same or similar conclusions.

The value of this information to GEH would be lost if the information were disclosed to the public. Making such information available to competitors without their having been required to undertake a similar expenditure of resources would unfairly provide competitors with a windfall, and deprive GEH of the opportunity to exercise its competitive advantage to seek an adequate return on its large investment in developing these very valuable analytical tools.

I declare under penalty of perjury that the foregoing affidavit and the matters stated therein are true and correct to the best of my knowledge, information, and belief.

Executed on this 30th day of December 2008.

David H. Hinds
GE-Hitachi Nuclear Energy Americas LLC

ATTACHMENT 1

MFN 08-968

Technical Proceeding (ICONE 16-48410)

"Steam Dryer Acoustic Load Predictions in the Main Steam Line Break"

by Jin Yan et. al. of GEH

Proceedings of the 16th International Conference on Nuclear Engineering
ICONE16
May 11-15, 2008, Orlando, Florida, USA

ICONE16-48410

STEAM DRYER ACOUSTIC LOAD PREDICTIONS IN THE MAIN STEAM LINE BREAK EVENT

Jin Yan Francis Bolger

Guangjun Li Weimin Dai Lev Klebanov

GE Hitachi Nuclear Energy
3901 Castle Hayne Road,
Wilmington, NC, 28402, U.S.A.

ABSTRACT

In nuclear reactor design, significant acoustic pressure loads impact the steam dryer hood as a result of the main steam line break outside containment (MSLB) event. When a main steam line breaks, it is assumed that the pipe instantaneously breaks completely open to the ambient environment (double-ended guillotine break). Due to the huge pressure difference between the inside of the reactor pressure vessel (RPV) and surrounding ambient environment, a shock wave will form at the break point and burst into the surrounding environment. At the same time, an expansion wave will travel upstream through the main steam line to the RPV, which results in a pressure reduction on the outside of the steam dryer hood. This expansion wave will create a substantial pressure difference between the two sides of the steam dryer hood with a resultant high stress on the hood. This differential pressure load is the acoustic load used in the structure design evaluations for this event.

A key design basis requirement for the steam dryer is to maintain structural integrity during transient, and accident conditions. Demonstration that the steam dryers meet this design basis requires a calculation of the magnitude of the acoustic load on the steam dryer during a MSLB. In this study, Computational Fluid Dynamics (CFD) is used as an alternate calculation method to investigate the phenomenon of MSLB. Transient simulations with fine time steps were carried out.

The results show that CFD is a useful tool to provide additional information on the acoustic load as compared to the traditional methods. From the CFD results, the minimum pressure value and its distribution area at different flow times was identified. Through the modeling, an understanding of the detailed transient flow field, particular the acoustic pressure field near the dryer hood during the MSLB was achieved.

INTRODUCTION

In a typical Boiling Water Reactors (BWR) RPV as shown in Figure 1, there are steam separators and steam dryers. At the top of the RPV, it is the steam dome. The steam dryer is made of banks of steam separating vanes and potentially perforated plates, with the dryer skirt and hoods directing the steam flow from the separators through the banks. The coolant (saturated water) is transformed into steam by the fission energy in the reactor core. The low quality steam, which is a mixture of water droplets and steam, goes through the steam separator where most of the water is separated from the steam. The moist steam then enters the steam dryer from the bottom where the steam is directed through separating vanes and the water droplets separated. The high quality steam exits upward from the steam dryer into the steam dome in the vessel head region. The steam then turns downward from the steam dome and enters the main steam line as shown in Figure 2. The main steam lines are connected to the steam turbines.

The general design criteria for power reactors require that the reactor internals maintain structural integrity, be able to withstand the effects of a breach in the reactor coolant pressure boundary up to the largest pipe of the reactor coolant system and perform their intended safety functions (e.g., maintaining the core geometry in a configuration that allows for reactor shutdown and cooling). The steam dryer is not a safety component, nor does it perform any safety functions. However, it must be shown that the dryer will maintain its

structural integrity under these pipe break conditions and not generate loose parts that may interfere with the operation of any safety system.

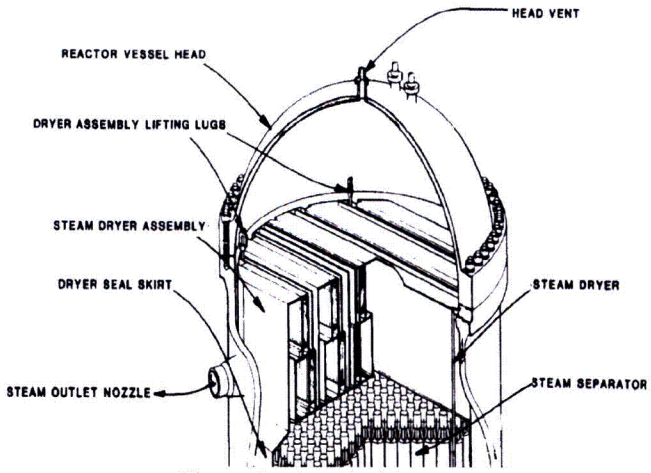

Figure 1 – A typical BWR4

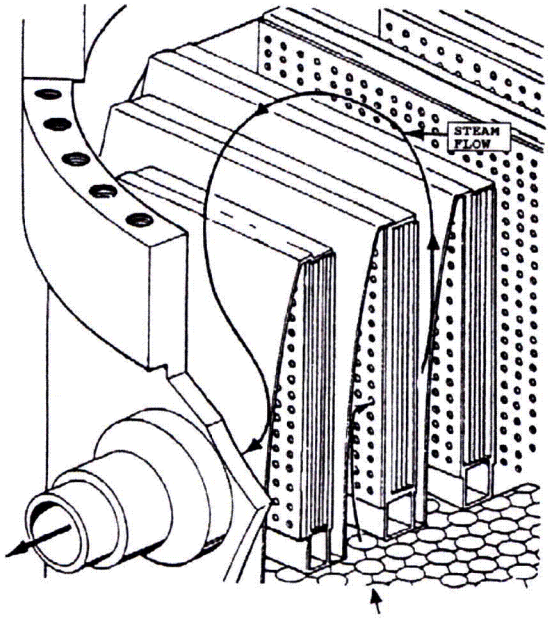

Figure 2 – Steam flow in a steam dryer

The MSLB Outside Containment event postulates a large steam line outside the containment and imposes the largest transient pressure loads on the dryer. It is assumed that the steam line instantaneously and circumferentially breaks at a location downstream of the isolation valve outside the containment boundary. A MSLB is postulated without the cause being identified. These lines are designed to high quality engineering codes and standards, and to seismic and environmental requirements. However, for the purpose of evaluating the consequences of a postulated large steam line rupture, the failure of a main steam line is assumed to occur.

When a MSLB occurs, the breaking point is completely open to the ambient environment (guillotine break). The normal operating pressure in the RPV is greater than 1000 psi. The MSLB creates a substantial pressure difference at the break location. The pressure difference will generate a shock wave and an expansion wave. The expansion wave will travel upstream into the RPV and reduce the pressure on the outside of the dryer hood. With the pressure inside the dryer hood still high, a substantial pressure difference across the hood will be created. The pressure difference could cause significant damage to the dryer hood. Therefore, the steam dryer must be designed to withstand the structural loads that result from this differential pressure. Traditionally, GE Hitachi Nuclear Energy has been using an in-house method and TRACG, which is a best-estimate thermal hydraulic code developed by GE Hitachi Nuclear Energy, to predict the pressure differential resulting from the MSLB event. It was thought that the transient behavior in the MSLB could be captured in more detail by using modern CFD. However, it is a challenge to accurately model the highly compressible flow, especially the very complex nature of the behavior of the non-linear expansion wave propagation in such a large domain. CFD was also used to provide an alternate calculation to TRACG for the maximum pressure drop across the dryer hood. In this paper, the CFD approach and the results will be discussed.

TECHNICAL APPROACH

In this study, a commercial 3 dimensional finite volume CFD code (CFX 10.0) was used. The code is a pressure based coupled code. When dealing with highly compressible flow with shock and expansion waves involved, it is desirable to use a density-based solver. However, it was thought that by using good quality hex mesh and appropriate time step size a reasonably accurate solution could be achieved.

CODE VALIDATION

In order to validate the proposed technical approach, the first task of this project was to validate the approach using a simple Riemann problem with a 3D shock tube. The tube has a diameter of 0.61 m and length of 6.1 m.

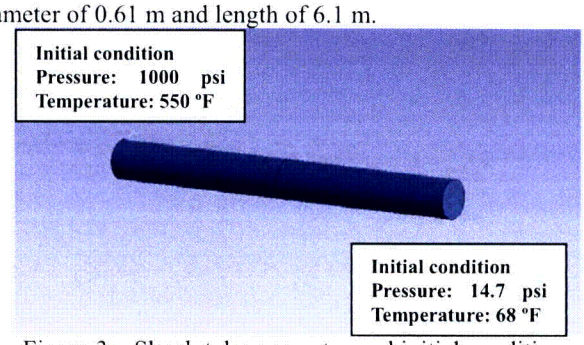

Figure 3 – Shock tube geometry and initial conditions

The initial condition of the shock tube is shown in Figure 3. The left half of the tube is filled with air at a pressure of 1000psi and right half is filled with air at a pressure of 14.7psi. The geometry is meshed with hexahedral elements using ICEM v 11.0 software package. A transient simulation with a time step of 4e-6 second was carried out. The time step was determined based on the time it takes the sound wave to travel one computational cell. The results are compared to the predictions from more precise numerical simulations. The numerical method in [1] was employed to simulate this Riemann problem with 1-D assumptions, which has the same initial conditions as the present test case discussed above. The High-order Characteristic-based Method (CBM) was developed in [1] to capture the moving shock and expansion waves. Three parameters distribution, pressure, density, and Mach number along the center axis are compared in Figure 4 through Figure 6.

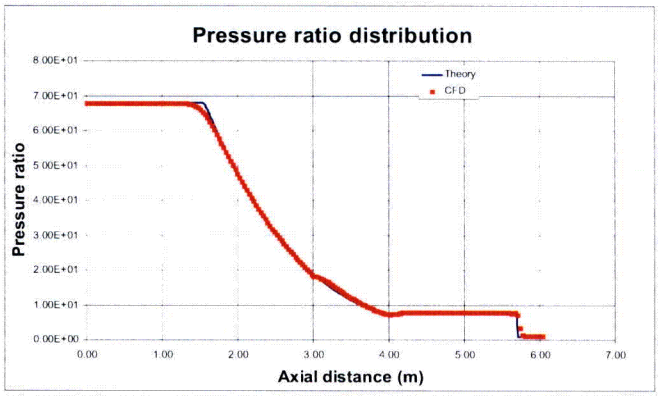

Figure 4 – Pressure ratio distribution

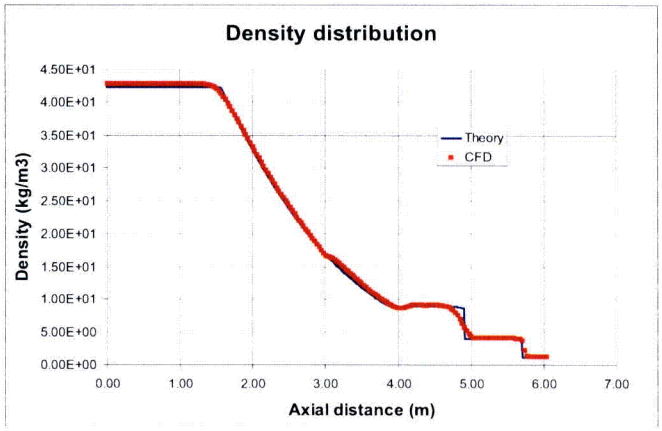

Figure 5 – Density distribution

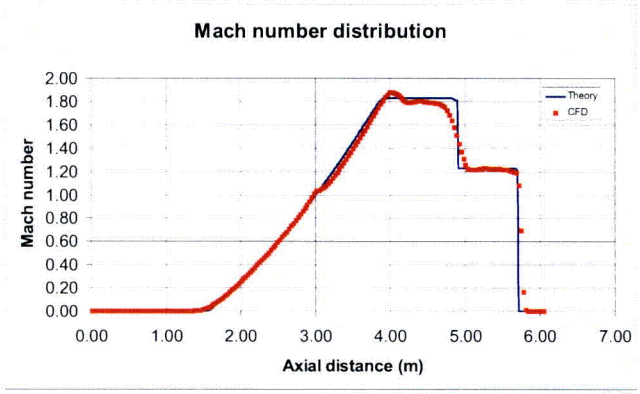

Figure 6 – Mach number distribution

From the pressure distribution in Figure 4, it can be seen that the CFD results accurately predict the pressure variation. The density distribution in Figure 5 shows a good agreement with the [1] solutions. However, the step change in the pressure, which represents the shock front location, predicted by CFD is not sharp enough. A refinement of the mesh at the locations with large density gradient will certainly help to improve the results. The Mach number distribution predicted by CFD in Figure 6 shows a good agreement with [1] solutions. From the above results, the CFD code and the technical approach are validated and therefore can be employed for the study of MSLB as an alternate calculation for TRACG verification in this area.

GEOMETRY AND MESH

The focus of the research is on the BWR configurations designed by GE Hitachi Nuclear Energy. In this paper, the geometry and dimensions for a generic BWR4 were used for investigation. The geometry contains half of the RPV and two main steam lines. Inside the RPV, two banks of dryers are included. The shroud, the down comer region, and the cover plate are represented in the geometry too. The steam lines are assumed to be straight. This represents the worst scenario so that conservative results can be produced. The flow limiters are also included in the steam lines as shown in Figure 7. In order to simulate the instantaneous break of one steam line, a large cylindrical fluid volume representing the discharge zone was added to the end of one steam line.

The geometry was created in ICEM v11.0 software package. A computational mesh with unstructured hexahedral elements was created. In order to minimize the numerical errors, only hexahedral cells were used. The mesh sizes near all walls are set to be small enough to employ the low Reynolds number turbulence model. On the steam line, a constant spacing, which is the same as the size used in the previous validation case, was used to accurately capture the wave motion. The total number of computational elements is 5.5 million.

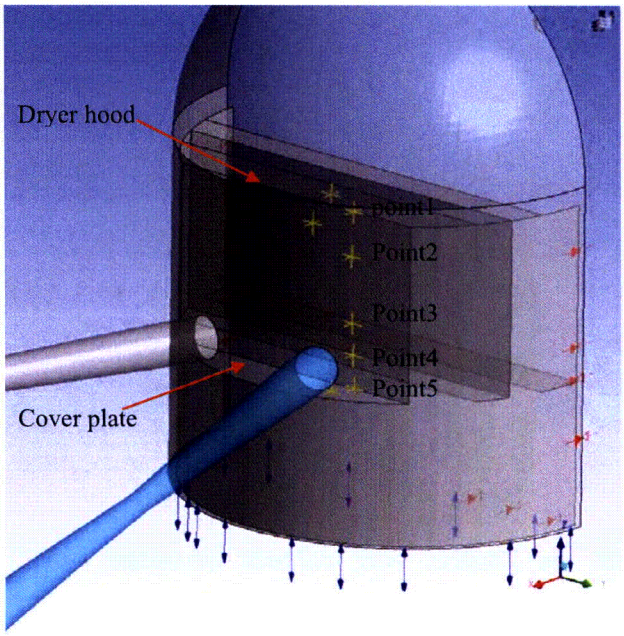

Figure 7 – A simplified BWR4 geometry and pressure monitor points on the dryer hood.

BOUNDARY CONDITIONS AND CALCULATION SETUP

The mesh was imported into the pre-processor. The water vapor is treated as an ideal gas. The bottom of the RPV is treated as a pressure inlet, where the total pressure and the total temperature were set as in the RPV operating conditions. The wall boundary was used at the down comer area, which is between the skirt and the vessel wall. At the end of the intact MSL, an open boundary with a slightly lower pressure and a constant temperature was used. At the boundaries of the discharge fluid zone, the open boundary with the standard ambient conditions was used.

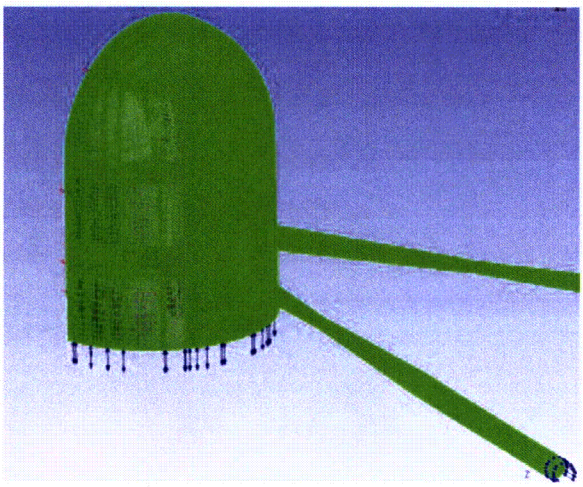

Figure 8 – Computational mesh

Since the calculation is transient, appropriate initial conditions of the fluid in the domain need to be set. It was proposed that a calculation of a standby break for MSLB would be the worst-case scenario. The standby condition assumes that the initial conditions of the fluid in the RPV and both steam lines have a constant pressure of 1025 psi and a constant temperature of 547 °F. The initial conditions in the discharge zone are the ambient conditions with the pressure of 14.7 psi and the temperature of 68 °F. The k-ω SST model developed by Mentor [3] was used as the turbulence model. High Resolution Scheme was used for the advection term. A time step of 4e-6 second was used with the second order numerical schemes. The time step size was determined based on the time it takes the sound wave to travel one computational cell.

CALCULATION AND PRESSURE MONITORS

The calculation was carried out on 35 processors in parallel. It took 14 days for the calculation to complete. During the calculation, the static pressure is monitored at on the cover plate, the outer side of the dryer hood, the top of the dryer, and the inner side of the dryer hood, as shown in Figure 9. The locations of those monitor points, Point 1 to Point 5, are shown in Figure 7. In addition, the maximum pressure on the dryer hood, the minimum pressure on the dryer hood, the averaged pressure on the dryer hood are also monitored at each time step as shown in Figure 10. The monitored locations are shown in Figure 7. The calculation was stopped when the pressure on the outer side of the dryer hood started to increase, indicating that the acoustic wave has passed.

CFD RESULTS AND DISCUSSIONS

At the beginning of the main steam line break, shock waves start forming at the break location. The shape of the shock waves changes rapidly and then settles into a quasi-steady shape as shown in Figure 11.

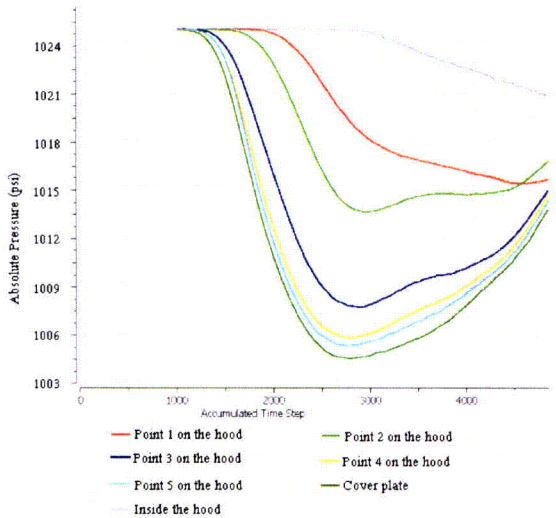

Figure 9 –History of the static pressure of the monitor points

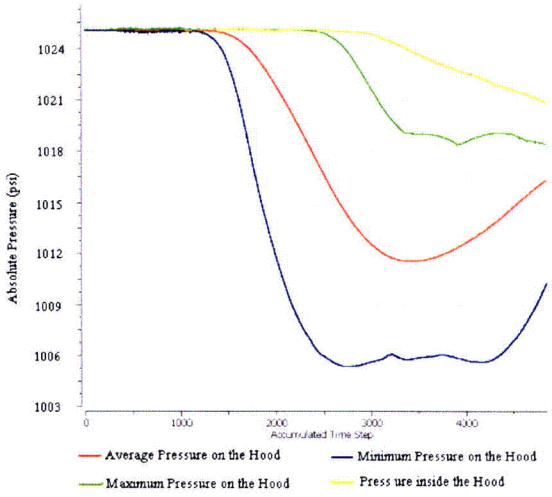

Figure 10 – History of the static pressure on the dryer hood

The static pressure on the outside of the dryer hood and the inside of the dryer hood is displayed in Figure 9. It can be seen that the pressure on those locations remained constant before the expansion wave front entered the RPV. The pressure on the cover plate, where it is closest to the steamline nozzle, started decreasing rapidly before all the other points. The sequence of the pressure change on the monitor points is decided by the monitor locations as shown in Figure 7. It indicates that the expansion wave front first hit the cover plate and then traveled up to the top of the dryer. The pressure variations on the dryer hood and the cover plate show that, at each monitor point, there is a minimum pressure at a certain flow time.

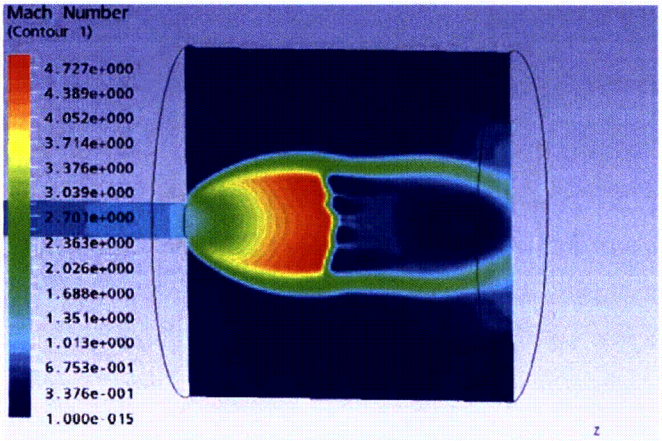

Figure 11- Mach number distribution 0.0251 second after the break at the broken location

The grey line on Figure 9 and the yellow line on Figure 10 show the pressure history at the inside of the pressure hood. The maximum pressure difference between the inside of the hood and the outside of the hood indicates the highest stress situation. In Figure 10, the time history of the minimum pressure on the outside of the dryer hood is displayed. The pressure drop (DP), which indicates the pressure difference between inside and outside the dryer hood, is displayed in Figures 12 & 13. The DP coefficients were obtained by normalizing the DP using the average dynamics pressure in the main steamline. From the CFD calculations, the maximum DP coefficient on the dryer hood caused by the MSLB is 3.17. However, from the DP coefficient plot of a monitor point on the cover plate in Figure 13, it can be found that the DP coefficients on the cover plate are higher than those on the outside of the dryer hood. The maximum DP coefficient on the cover plate from the CFD prediction is 3.67. It shows that the cover plate experienced more stress than the dryer hood. There are two peaks for the monitor point 3 in Figure 13. The second peak indicates the reflection of the expansion wave between the dryer hood and the RPV wall. The maximum stress point is shown in Figure 14. The maximum DP value from CFD is comparable to the value produced by TRACG. However, CFD provides more detailed flow information such as the location of the maximum DP point, the wave reflection time, etc. Due to it's proprietary nature, the TRACG data is not presented here.

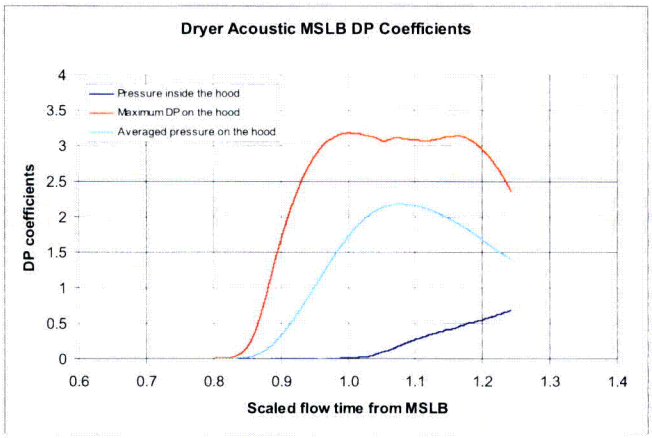

Figure 12-DP history on the dryer hood

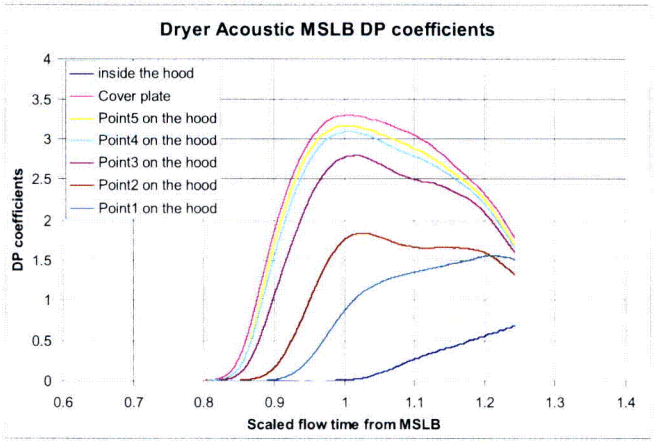

Figure 13-DP history on the monitor points

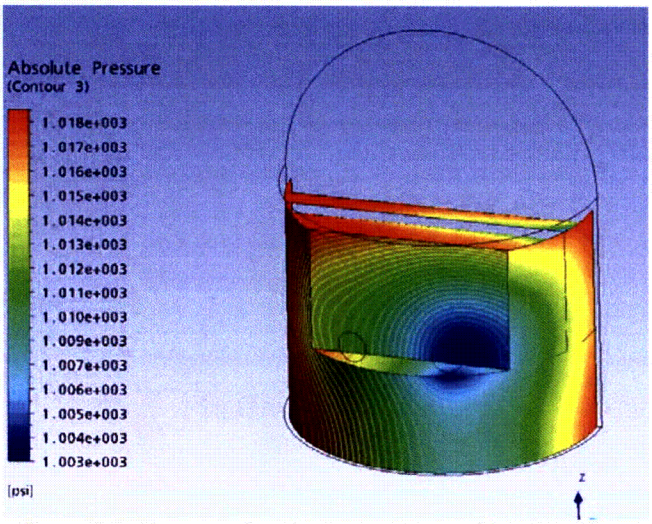

Figure 14 – Pressure distribution on the outside of the dryer hood

CONCLUSIONS

Transient CFD simulations of the Main Steam Line break event were completed on a half model of a BWR4 RPV. A single shock tube simulation was carried out to validate the accuracy of the CFD approach. A high fidelity mesh with all hexahedral cells was generated to minimize the numerical diffusion. The shock wave and the expansion wave development have been observed in the results. The maximum differential pressure across the dryer hood and the cover plate are reported. The differential pressure across the cover plate of the dryer is higher than that on the dryer hood. The reflection of the wave between the dryer hood and the vessel wall is captured by the CFD solution. Compared to the traditional methods, CFD can not only predict the maximum differential pressure, but also the location of where the maximum differential pressure is on the structure.

REFERENCES

[1] Nourgaliev, R.R., Dinh, T.N., Theofanous, T.G., "The Characteristics-Based Matching (CBM) Method for Compressible Flow With Moving Boundaries and Interfaces", Transactions of ASME: Journal of Fluids Engineering 126, pp.586-604, 2004.

[2] NUREG-0800, "STANDARD REVIEW PLAN", U.S. Nuclear Regulatory Commission, 2007.

[3] Menter, F.R., "Two-equation Eddy-Viscosity Turbulence Models for Engineering Applications", AIAA-Journal., **32**(8), 1994.